Theoretical and Applied Fracture Mechanics 107 (2020) 102519

Contents lists available at ScienceDirect

Theoretical and Applied Fracture Mechanics

journal homepage: www.elsevier.com/locate/tafmec

Correlation between real geometry and tensile mechanical behaviour for Ti6Al4V electron beam melted thin specimens

R. Sepe[a,*], S. Franchitti[b], R. Borrelli[b], F. Di Caprio[b], E. Armentani[c], F. Caputo[d]

[a] Dept. of Industrial Engineering, University of Salerno, Via G. Paolo II, 132 - 84084 Fisciano, Italy
[b] CIRA, Italian Aerospace Research Centre, Structural and Material Department, Via Maiorise, 81043 Capua, Italy
[c] Dept. of Chemical, Materials and Production Engineering, University of Naples Federico II, P.le V. Tecchio, 80, 80125 Naples, Italy
[d] Dept. of Engineering, University of Campania "Luigi Vanvitelli", Via Roma 29, 81031 Aversa, Italy

ARTICLE INFO

Keywords:
Additive manufacturing
EBM
Titanium Ti6Al4V
Tensile mechanical properties

ABSTRACT

The Electron Beam Melting (EBM) is an Additive Layer Manufacturing (ALM) technique used to directly manufacture 3D functional parts from metal powder, selectively melted, layer by layer, by an electron beam according to a geometry defined by a CAD model. The EBM technology allows benefitting from countless advantages: material waste reduction, easy manufacturing of complex shapes, lead time reduction, etc; on the other hand the EBM process is typically associated with lower resolutions and higher surface roughness (R_a = 25–30 µm) compared to similar laser based powder bed metal processes.

Therefore the surface morphology may be a critical issue for the structural integrity of components made in EBM and used in-service in their "as built" condition, i.e. with the characteristic surface released by the process.

This study evaluates surface morphology and tensile properties of Ti6Al4V specimens of varying nominal thickness (1–5.0 mm), made by using EBM process with a layer thickness of 50 µm. The aim is therefore to investigate how the surface morphology and the tensile properties are affected by the nominal thickness of the component.

1. Introduction

In the industrial production environment, in the last years, the Additive Layer Manufacturing technologies (ALM) are taking an increasingly important role. These innovative technologies allow the production of a layer-by-layer component, with the progressive adding of material. These are production processes that have been developed for a long time in the field of rapid prototyping, but only in recent years have been massively applied to industrial production [1–5].

Electron Beam Melting (EBM) is an ALM technology developed by the Swedish company Arcam AB Corporation, which commercialized the first machines in 1997 to provide efficient solutions for the production of metal components [6,7]. The EBM was developed by the company to process materials, such as titanium alloys, that require high process temperatures being difficult-to-machine through traditional processing technologies. The final goal is to economically produce demanding applications such as low-pressure turbine blades and structural aerospace components [8–10]. EBM employs the energy of an electron beam to selectively melt a layer of metal powders, creating a three-dimensional layer-by-layer component. During the EBM process, each layer of the component is melted in two phases referred to as contouring and hatching. Contouring, which is used to improve the surface finish, melts the outlines of the layer and it is characterized by a constant beam power and a constant scanning speed. Generally it is performed in two steps, spaced by an offset, called inner and outer contouring. The hatching is used to melt the inner part of the layer and unlike the contouring phase, the beam power and the scanning speed are continuously varied according to the thermal conditions of the melting pool which are function of the geometry of the printed component.

EBM and in general the additive technologies potentially offer to designers and technologists numerous advantages such as the reduction of the lead-time of new product and the possibility of producing any kind of complex shape. However, the production process is affected also by some limitations that mainly concern surface finish and dimensional accuracy of the components. In particular, for EBM, the problem of dimensional accuracy is due to some process factors such as the thermal shrinkage, the electron beam diameter and the random average diameter value of the powders used. On the other hand, as regards to the surface roughness, it has been widely studied that the process

* Corresponding author.
E-mail address: rsepe@unisa.it (R. Sepe).

https://doi.org/10.1016/j.tafmec.2020.102519
Received 29 January 2020; Received in revised form 6 February 2020; Accepted 6 February 2020
Available online 07 February 2020
0167-8442/

parameters and the reduction of the thickness of the components are the main affecting factors [11,12].

In a previous work [13], Sepe et al. found that there is not substantial difference between the Young's modulus of the specimens made with contouring theme and that one of specimens made with contouring and hatching theme when the specimens have the same thickness. On the contrary, other mechanical properties vary with the thickness, because of the high roughness of the components made by EBM which reduces the effective cross section.

Nowadays, the high roughness of the components made by EBM and the difference in size of the printed parts with respect to the size of the CAD model, involve high approximation on the mechanical behaviour of parts made by EBM that are employed in-service without any post manufacturing finish process, like trusses in a lattice structures or thin-walled components that have a thickness lesser than that of a standard testing coupon used in mechanical testing. Therefore, it is important to investigate the mechanical behavior of EBM built parts with respect to the surface condition and thickness dependency.

In this paper, an experimental study was carried out in order to evaluate the surface morphology and the tensile properties of Ti6Al4V samples of varying nominal thickness (1.0–5.0 mm) manufactured using the EBM process. The purpose was to investigate how the surface morphology and tensile properties are affected by the component size.

2. Materials and methods

The Ti6Al4V alloy, in the raw state, used in this study for the EBM process, is produced and distributed by Arcam AB Corporation in the form of powders, with a nominal diameter in the range of 45–100 µm obtained by atomization process. The chemical composition in wt% of powders is reported in Table 1.

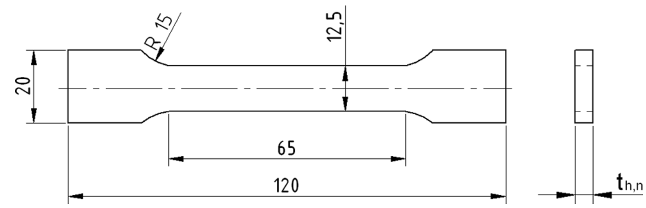

Fig. 1. Shapes and sizes of specimens.

Table 2
Nominal sizes and number of specimens.

Batch	Number of specimens	Thickness $t_{h,n}$ [mm]	Width W_n [mm]	Nominal area A_n [mm^2]
A1	5	1	12.5	12.5
A2	5	2	12.5	25.0
A3	5	3	12.5	37.5
A4	5	5	12.5	52.5

Table 3
Real sizes of cross section of specimens.

Batch	Number of specimens	Mean Meas. thickness $t_{h,meas.}$ [mm]	Mean Meas. width $W_{meas.}$ [mm]	Mean Meas. area $A_{meas.}$ [mm^2]
A1	5	1.189	12.571	14.947
A2	5	2.118	12.503	26.481
A3	5	3.067	12.505	38.354
A4	5	5.046	12.672	63.943

Table 1
Chemical composition of powder (wt%).

Material	Al	V	Fe	O	N	H	C	Ti
Ti6Al4V Used Powder [%]	6.38	4.14	0.19	0.14	0.02	< 0.003	0.01	Balance
Required [%] ASTM F2924	5.5 ÷ 6.75	3.5 ÷ 4.5	< 0.3	< 0.2	< 0.05	< 0.01	< 0.1	Balance

Specimens with four different thicknesses (1.0 mm, 2.0 mm, 3.0 mm and 5.0 mm) were manufactured using the ARCAM A2X available at the Italian Aerospace Research Centre (CIRA). Standard process themes, developed by ARCAM AB for the Ti6Al4V Titanium alloy with a layer thickness equal to 50 µm, were used in this study. The process was carried out in vacuum (in the chamber, from 5×10^{-3} mbar at the start to 2×10^{-5} mbar at the end of the process).

Shape and nominal sizes of the specimens are shown in Fig. 1 and Table 2.

2.1. Static tests

Static tensile tests were carried out according to ASTM E8 [14] by electromechanical testing system Zwick 250 with a load cell capacity of 250 kN, the strains during the tests were measured by means of an extensometer.

The specimens were tested under displacement control with a crosshead speed $v = 1.86$ mm/min, up to failure. The dimensions of the cross sections of the specimens were measured using calipers on the as fabricated surfaces. The sizes of specimens measured with calipers are reported in Table 3. The measured dimensions were obtained by arithmetic average of the measured dimensions of specimens belonging to the same batch.

2.2. Microscopic analyses

In order to evaluate the effective cross section area of the specimens, above all for the thinner ones, three further specimens having the same cross section of the tensile test specimens (12.5 mm as width and different thicknesses) were manufactured in the same job and thus by using the same process parameters. The nominal dimensions and the identification label of the specimens are reported in Table 4.

Table 4
Nominal sizes of samples used in microscopic analyses.

Specimen	Length L [mm]	Width W_n [mm]	Thickness $t_{h,n}$ [mm]	Nominal area A_n [mm^2]
S1	20	12.5	1	12.5
S2	20	12.5	2	25.0
S3	20	12.5	3	37.5

The specimens were cross-sectioned by using a low speed, water cooled, sectioning machine REMET MT60 and submitted to microscopic analysis. From the sectioning, six samples were obtained (two for each specimen).

Each sample was mounted in the resin and grinded with 180 grit papers. The grinded samples were inspected with stereo-microscope LEICA MZ12 with a magnification of 20X. The images of the cross sections were acquired by the digital camera LEICA MC 190 HD and elaborated by the software LAS EZ and MATLAB in order to measure the effective cross section area of the specimens.

The evaluation of the effective cross section area of the specimens is fundamental for the interpretation of the results of the experimental tensile test.

3. Results and discussion

3.1. Static tests

In Table 5, the results of tensile tests are reported in terms of Young's modulus E, yield stress σ_y, ultimate tensile stress σ_r and percentage elongation Z with standard deviation (S), while in Fig. 2 the tipically stress vs. strain curves for each thickness are shown.

The experimental results show a strong dependence of the mechanical properties on the thickness. The specimens 1 mm thick have the lower values of the evaluated mechanical properties and this is due to the surface roughness of the specimens which reduces the cross section more than for the thicker specimens (as in the following it will be shown). This confirms the results of tensile tests of previous work [13].

Table 5
Experimental results of tensile tests.

Batch	E [MPa] (S)	σ_y [MPa] (S)	σ_r [MPa] (S)	Z [%] (S)
A1	92,607 (3119)	645 (9.2)	673 (9.6)	2.9 (0.7)
A2	114,979 (4890)	792 (4.7)	820 (11.2)	5.3 (0.3)
A3	119,590 (5331)	863 (5.9)	895 (4.8)	5.0 (0.9)
A4	120,880 (3753)	899 (10.3)	941 (5.7)	6.3 (0.9)

The Figs. 3–5 show the evaluated mechanical properties compared with respect to literature data [15], which can be considered as the tensile mechanical properties of the core (typical material). In fact, in their work Pirozzi et al. [15] obtained such mechanical properties from machined specimens in order to remove the surface roughness. The literature values are represented with blue line in the figures (dash dot blue lines represent the statistical distribution in terms of standard deviation).

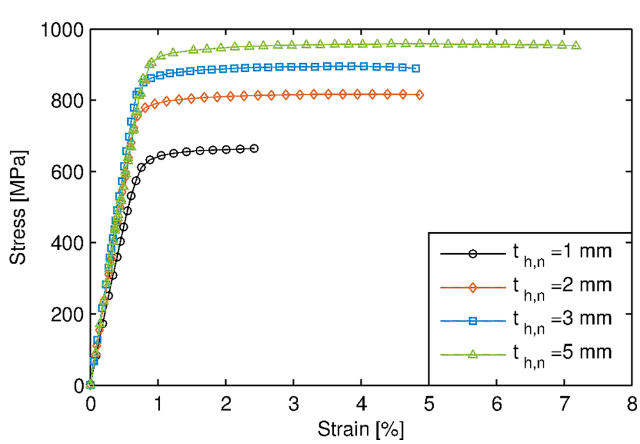

Fig. 2. Stress vs. strain curves.

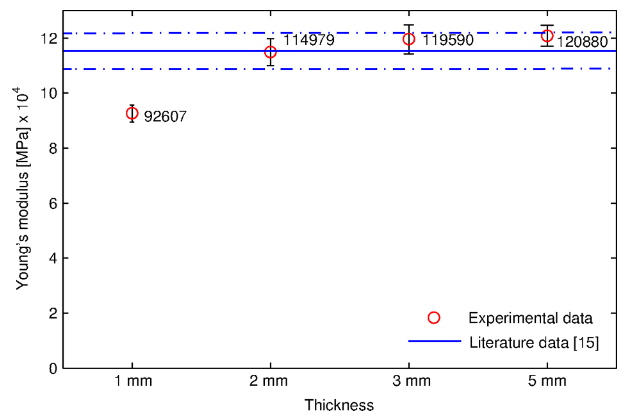

Fig. 3. Young's modulus of specimens compared with literature data.

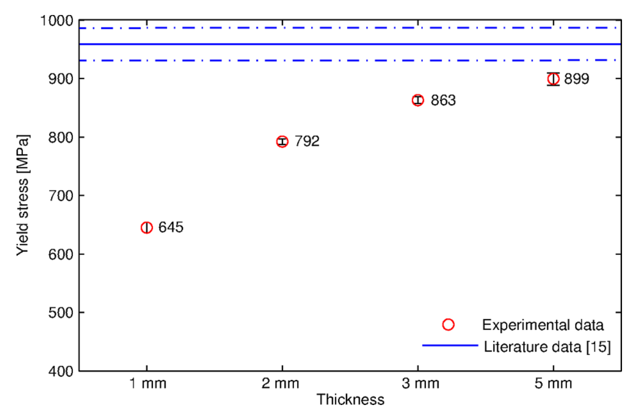

Fig. 4. Yield stress of specimens compared with literature data.

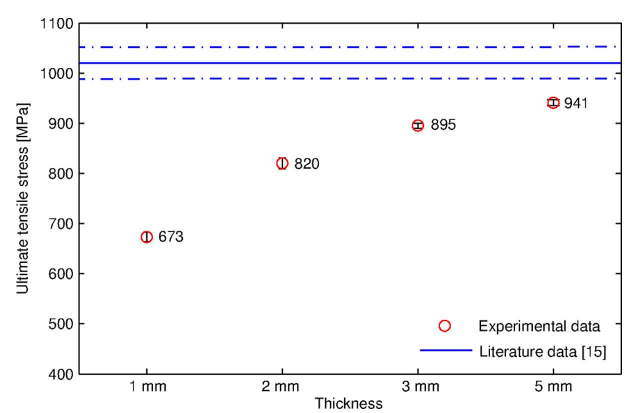

Fig. 5. Ultimate tensile stress of specimens compared with literature data.

In the case of yield stress and ultimate tensile stress (Figs. 4 and 5) these mechanical properties tend towards to the material characteristic value confirming that the surface roughness reduces the mechanical properties, especially in thin specimens, where the cross-section area reduction, in percentage, is more critical. While the value of Young's modulus reaches a reference value of about 120,000 MPa already when the thickness of specimen is 3 mm, this means that for values of thickness higher than 3 mm the surface roughness does not influence the Young's modulus (Fig. 3). Moreover, this value is in good agreement with the value obtained by Pirozzi et al. [15] with a difference of only 5% which is within a normal statistical dispersion of data.

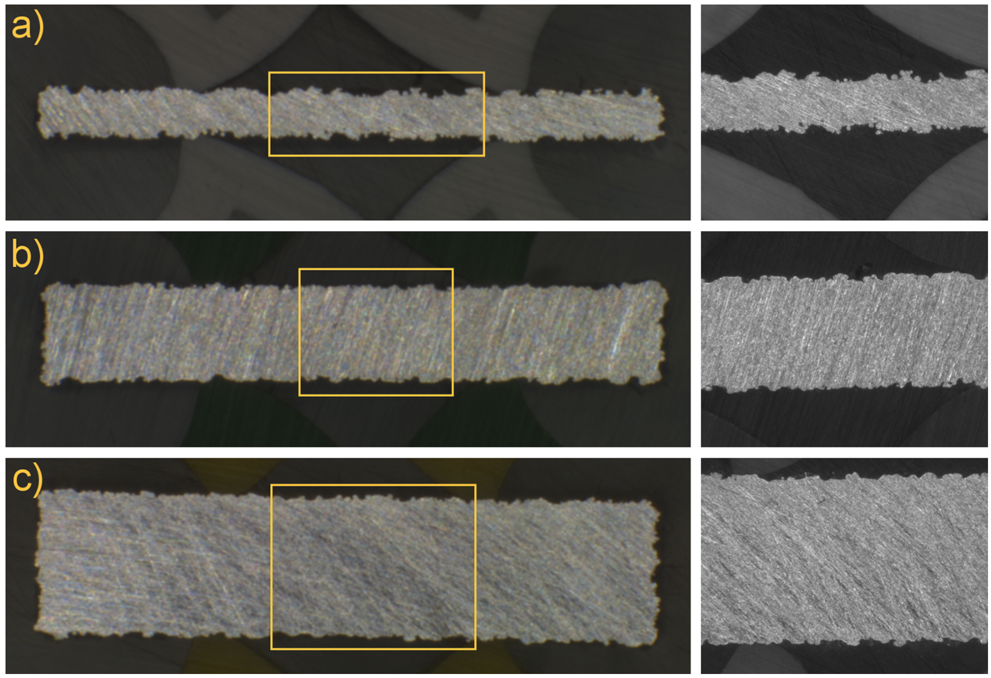

Fig. 6. Cross section of the specimens obtained by microscopic analyses: (a) 1 mm tick; (b) 2 mm tick; (c) 3 mm tick.

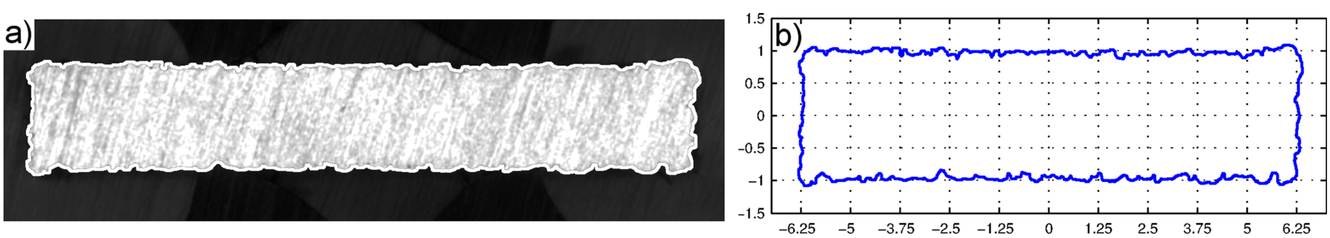

Fig. 7. (a) image of cross section processed by software LAS EZ; (b) frontier of the cross section.

3.2. Microscopic analysis

Fig. 6 shows the cross sections of the specimens. It is possible to observe as the external surface of the specimens is very irregular due to the roughness. This involves that the effective cross section area is different, in particular lower (especially for the specimen 1 mm thick) than the measured area $A_{meas.}$ used to calculate the mechanical properties and reported in Table 3.

The images of cross sections (Fig. 7a) were acquired by digital camera LEICA MC 190 HD and elaborated with software LAS EZ in order to obtain the cross-section boundary (Fig. 7b).

After that the frontier of each cross section was elaborated with MATLAB, in order to obtain the effective area $A_{eff.}$ of each specimen (Fig. 8).

The results obtained by elaborating the images of the specimen cross sections with different thickness are summarized in Table 6. Also, in Table 6 the nominal area A_n, the measured area $A_{meas.}$ and the difference in percentage between the measured area $A_{meas.}$ and effective area $A_{eff.}$ are reported.

The results, reported in Table 6, show that the difference in percentage between measured area $A_{meas.}$ and effective area $A_{eff.}$ decreases as the thickness of specimen increases, this means that the roughness has high influence on the effective area of the specimen when it is thinner.

Therefore, by using the effective area A_{eff} instead of the measured area $A_{meas.}$ (Table 6), it is possible to recalculate the tensile mechanical properties of the specimens. In particular, the reduction percentage of 5 mm specimen sectional area was calculated by extrapolation from the data reported in Table 6 and it was estimated equal to 2.17%.

The recalculated properties are reported in Table 7 and tend to the

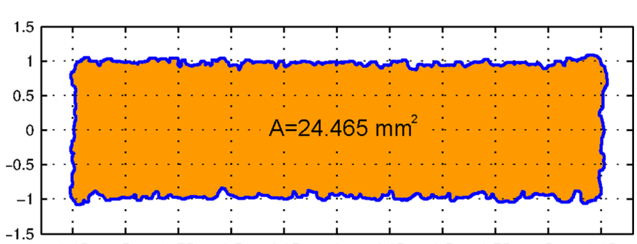

Fig. 8. Effective area of cross section $A_{eff.}$ of specimen S2_2.

Table 6
Effective area $A_{eff.}$ obtained by microscopy analyses.

Specimen	A_n. [mm^2]	$A_{meas.}$ [mm^2]	$A_{eff.}$ [mm^2]	$(A_{meas.} - A_{eff.})\cdot 100/A_{eff.}$ [%]	Average of difference for each specimens [%]
S1_1	12.50	14.997	12.235	22.57	23.03
S1_2	12.50	14.997	12.145	23.48	
S2_1	25.00	26.482	24.586	7.71	7.98
S2_2	25.00	26.482	24.465	8.24	
S3_1	37.50	38.354	36.686	4.55	4.68
S3_2	37.50	38.354	36.590	4.82	

Table 7
Experimental results of tensile tests recalculate with effective area.

Batch	E (MPa) (S)	σ_y (MPa) (S)	σ_r (MPa) (S)
A1	113,932 (3119)	794 (9.2)	828 (9.59)
A2	124,151 (4890)	855 (4.7)	885 (11.2)
A3	125,191 (5331)	903 (5.9)	937 (4.8)
A4	123,503 (3753)	919 (10.3)	961 (5.7)

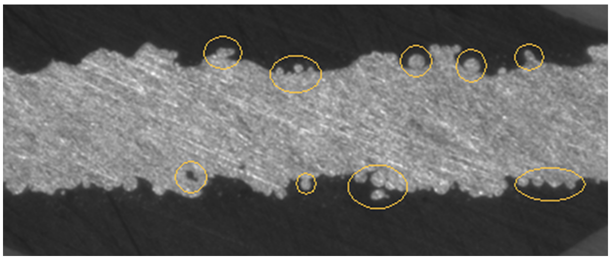

Fig. 9. Voids and ridges of material on the surface of specimens tick = 1 mm.

values obtained by Pirozzi et al. [15] with a difference lower than 8%. Moreover, from results reported in Table 7 it possible to state that the recalculated Young modulus E of specimens is about the same for all specimens and therefore the difference of results reported in Table 5 is due only to the value of the area of cross section used to calculate it. The lower values of mechanical properties of batch A1 can be due to the presence of voids in the cross section or higher surface roughness of the specimens that produces ridges of material on the surface of specimens that does not collaborate to strength of specimens (Fig. 9).

4. Conclusions

From the results obtained by the tests on specimens with different thickness there is a strong influence of specimens dimension on all the considered tensile mechanical properties (Young's modulus, yield stress and ultimate tensile stress).

Such mechanical properties are lower for the thinner specimens and this is due to the fact that the reduction of the actual cross section (in percentage) due to surface roughness is greater for these specimens as confirmed by the microscopic analyses. In fact, if the effective area of specimens is considered, the mechanical properties of materials are close to the values present in literature for machined specimens. This influence is stronger when the thickness of specimens is lower than 3 mm.

Therefore, it is necessary that designers use appropriate values of the material mechanical properties, which take into account the effective resistance of the component, especially in design of parts that will be used in-service in their "as built" state and having thin dimensions.

CRediT authorship contribution statement

R. Sepe: Writing - original draft, Investigation, Methodology. **S. Franchitti:** Resources. **R. Borrelli:** Conceptualization, Resources. **F. Di Caprio:** Resources, Writing - review & editing. **E. Armentani:** Data curation, Writing - review & editing. **F. Caputo:** Supervision.

Declaration of Competing Interest

The authors declare that they have no known competing financial interests or personal relationships that could have appeared to influence the work reported in this paper.

Acknowledgment

Authors acknowledge Dr. Andrea Vigliotti and Dr. Angela Ferrigno for their support during the microscopic analysis of samples.

Appendix A. Supplementary material

Supplementary data to this article can be found online at https://doi.org/10.1016/j.tafmec.2020.102519.

References

[1] L.E. Murr, E.V. Esquivel, S.A. Quinones, S.M. Gaytan, M.I. Lopez, E.Y. Martinez, F. Medina, D.H. Hernandez, E. Martinez, J.L. Martinez, S.W. Stafford, D.K. Brown, T. Hoppe, W. Meyers, U. Lindhe, R.B. Wicker, Microstructures and mechanical properties of electron beam-rapid manufactured Ti-6Al-4V biomedical prototypes compared to wrought Ti-6Al-4V, Mater. Charact. 60 (2009) 96–105.

[2] A. Safdar, L.Y. Wei, A. Snis, Z. Lai, Evaluation of microstructural development in electron beam melted Ti-6Al-4V, Mater. Charact. 65 (2012) 8–15.

[3] L. Facchini, E. Magalini, P. Robotti, A. Molinari, Microstructure and mechanical properties of Ti-6Al-4V produced by electron beam melting of pre-alloyed powders, Rapid Prototyping J. 15 (2009) 171–178.

[4] N. Hrabe, T. Quinn, Effects of processing on microstructure and mechanical properties of a titanium alloy (Ti–6Al–4V) fabricated using electron beam melting (EBM), Part1: Distance from build plate and part size, Mater. Sci. Eng. A 573 (2013) 264–277.

[5] G. Welsch, E.W. Collings, R. Boyer, Materials Properties Handbook: Titanium Alloys, ASM International, 1994.

[6] X. Gong, T. Anderson, K. Chou, Review on powder-based electron beam additive manufacturing technology, Manuf. Rev. 1 (2014) 1–10.

[7] C. Koerner, Additive manufacturing of metallic components by selective electron beam melting - a review, Int. Mater. Rev. 61 (2016) 361–377.

[8] ARCAM, «Arcam A2X - For aerospace production and materials R&D, ».

[9] J. Parthasarathy, B. Starly, S. Raman, A. Christensen, Mechanical evaluation of porous titanium (Ti6Al4V) structures with electron beam melting (EBM), J. Mech. Behav. Biomed. 3 (3) (2010) 249–259.

[10] G. Baudana, S. Biamino, D. Ugues, M. Lombardi, P. Fino, M. Pavese, C. Badini, Titanium aluminides for aerospace and automotive applications processed by Electron Beam Melting: Contribution of Politecnico di Torino, Metal Powder Report 71 (3) (2016) 193–199.

[11] A. Safdar, H.Z. He, L.-Y. Wei, A. Snis, L.E. Chavez de Paz, Effect of process parameters settings and thickness on surface roughness of EBM produced Ti-6Al-4V, Rapid Prototyp. J. 18 (5) (2012) 401–408.

[12] M. Koike, K. Martinez, L. Guo, G. Chahine, R. Kovacevic, T. Okabe, Evaluation of titanium alloy fabricated using electron beam melting system for dental applications, J. Mater. Process. Tech. 211 (2011) 1400–1408.

[13] R. Sepe, F. Di Caprio, S. Franchitti, R. Borrelli, C. Pirozzi, A. Langella, G. Ippolito, F. Caputo, The effect of the contour on the mechanical properties of the Ti6Al4V Electron Beam Melted, in: Proceedings of The First European Conference on Structural Integrity of Additively Manufactured Materials (ESIAM19) 9–11 September 2019, Trondheim, Norway.

[14] ASTM E8/E8M-16a, Standard Test Methods for Tension Testing of Metallic Materials, ASTM International, West Conshohocken, PA, 2016.

[15] C. Pirozzi, R. Borrelli, S. Franchitti, F. Caiazzo, V. Alfieri, P. Argenio, Study on the factors affecting the mechanical behavior of electron beam melted Ti6Al4V, J. Mater. Eng. Perform. 26 (2017) 4491–4499.